Original Article

Eur J Breast Health 2026; 22(1): 44-53
DOI: 10.4274/ejbh.galenos.2025.2025-9-1

Predictive Value of Dimensional and Functional MRI Parameters on Mid-Treatment MRI for Pathologic Complete Response in Breast Cancer

Ahmet Bozer, Levent Altın, Hamza Eren Güzel
Department of Radiology, Ministry of Health İzmir City Hospital, İzmir, Türkiye

ABSTRACT

Objective: To evaluate the predictive performance of dimensional and functional magnetic resonance imaging (MRI) parameters obtained from mid-treatment breast MRI for forecasting pathologic complete response (pCR) in patients with locally advanced breast cancer (LABC) undergoing neoadjuvant chemotherapy (NAC).

Materials and Methods: Sixty-five women with LABC who underwent NAC followed by surgery were retrospectively included. Quantitative MRI parameters—including % change (Δ%) in longest diameter, bidimensional size, tumor volume, apparent diffusion coefficient (ADC), and enhancement percentage (Epeak)—were calculated between pre- and mid-NAC MRI. Receiver operating characteristic (ROC) analysis and logistic regression were used to identify predictors of pCR. Logistic regression and ROC analysis (with DeLong's test) were used to assess associations with pCR and compare area under the curves (AUCs).

Results: pCR was achieved in 19 of 65 patients (29%). Compared to non-pCR cases, patients with pCR showed significantly greater reductions in tumor size and Epeak, and larger increases in ADC value (all $p<0.05$). In multiple logistic regression, Δ% longest diameter >60% [odds ratio (OR)=7.1, $p = 0.008$] and Δ% ADC value ≥32% (OR=4.7, $p = 0.016$) remained statistically significant independent predictors of pCR. Δ% tumor volume >92% had the highest univariable AUC (0.754), while Epeak ≤21% showed perfect specificity but was excluded due to wide confidence intervals. Pairwise AUC comparisons showed no significant differences among Δ% longest diameter, bidimensional size, and tumor volume (all $p>0.05$).

Conclusion: Mid-treatment MRI biomarkers, particularly Δ% longest diameter and Δ% ADC value, are effective early predictors of pCR and may support individualized treatment strategies during NAC.

Keywords: Breast cancer; neoadjuvant chemotherapy; mid-treatment; magnetic resonance imaging; pathologic complete response.

Cite this article as: Bozer A, Altın L, Güzel HE. Predictive value of dimensional and functional MRI parameters on mid-treatment MRI for pathologic complete response in breast cancer. Eur J Breast Health. 2026; 22(1): 44-53

Key Points

- Mid-treatment magnetic resonance imaging (MRI) provides valuable early information for predicting pathologic complete response (pCR) during neoadjuvant chemotherapy in breast cancer.
- Δ% longest diameter >60% and Δ% apparent diffusion coefficient (ADC) value ≥32% were identified as independent predictors of pCR in multiple logistic regression (MLR).
- Δ% tumor volume showed the highest univariable area under the curves but was not retained in the MLR model due to collinearity.
- Functional (ADC) and dimensional (size-based) MRI parameters offered comparable diagnostic performance for pCR prediction.
- These non-invasive, easily obtainable imaging biomarkers may support early risk stratification and individualized treatment planning.

Introduction

Neoadjuvant chemotherapy (NAC) has become a cornerstone in the management of locally advanced breast cancer (LABC), enabling tumor downstaging, facilitating breast-conserving surgery, and offering an *in vivo* assessment of chemosensitivity prior to surgery. One of the critical surrogate endpoints used to evaluate NAC efficacy is the achievement of a pathologic complete response (pCR), which has been shown to correlate with improved long-term outcomes, particularly in human epidermal growth factor receptor 2 (HER2)-positive and triple-negative subtypes (1, 2).

Early prediction of pCR is critical for guiding treatment decisions, including de-escalation or intensification of therapy. Magnetic resonance imaging (MRI) has been shown to outperform conventional modalities such as mammography, digital breast tomosynthesis, and

Corresponding Author:
Ahmet Bozer MD; drahmetbozer@gmail.com

Received: 01.09.2025
Accepted: 26.09.2025
Epub: 23.10.2025
Online Publication Date: 25.12.2025

automated breast ultrasound, while emerging techniques like contrast-enhanced spectral mammography and positron emission tomography/MRI offer additional functional insights (3-6).

Among the various MRI time points, mid-treatment (mid-NAC) MRI, typically performed after 2 to 4 cycles of chemotherapy, provides a unique opportunity to assess early response and adapt treatment plans in real time (7, 8). This time point allows clinicians to evaluate early response and modify treatment plans accordingly, potentially avoiding unnecessary toxicity or surgical delays.

Building on this potential, several studies have evaluated the predictive value of MRI-derived quantitative parameters in predicting pCR to NAC in breast cancer patients. These parameters include not only morphologic features such as tumor diameter and volume but also functional measures like peak enhancement percentage (Epeak) and apparent diffusion coefficient (ADC) (7-10).

Tudorica et al. (8) demonstrated that early changes in functional MRI parameters after just one cycle of NAC were more effective in predicting pCR than conventional size-based criteria. Similarly, in a prospective study on inflammatory breast cancer, Le-Petross et al. (11) reported that mid-treatment median and mean ADC values were significantly associated with pCR, highlighting their potential as early imaging biomarkers. Despite these encouraging findings, the overall results remain heterogeneous, and there is still no consensus regarding the most reliable parameters or optimal cut-off values. Moreover, although mid-NAC MRI has attracted growing interest, the majority of existing research has focused on post-treatment imaging. Therefore, further validation in well-defined patient cohorts is needed to clarify the combined predictive value of morphologic and functional MRI biomarkers at the mid-NAC stage (4, 8).

Therefore, this study aims to evaluate the predictive performance of both morphologic and functional MRI biomarkers obtained at the mid-treatment stage for forecasting pCR in patients with LABC receiving NAC. By investigating multiple MRI-derived parameters, including tumor size, Epeak, and ADC, we seek to contribute to the development of reliable imaging-based predictors that can guide early treatment decisions.

Materials and Methods

Study Design and Patient Selection

This retrospective study was approved by the University of Health Sciences Türkiye, İzmir Bozyaka Training and Research Hospital Clinical Research Ethics Committee (approval date: 29/11/2023; decision no: 2023/197). Patients diagnosed with breast cancer at our institution between 2019 and 2021 were evaluated for eligibility. Inclusion criteria were as follows: receipt of NAC; availability of breast MRI at three distinct time points—prior to NAC (pre-NAC), mid-treatment (after the fourth chemotherapy cycle) (mid-NAC), and post-treatment (post-NAC); and subsequent surgery performed at our institution with pathological assessment of treatment response. Of the initially screened patients, those were excluded due to incomplete or prematurely terminated NAC or non-adherence to the treatment protocol (n = 5), lack of pre-treatment pathological confirmation at our institution (n = 2), absence of appropriately timed or technically adequate MRI examinations (n = 4), history of prior malignancy or cancer treatment (n = 1), or surgery performed outside our institution without pathological response evaluation (n = 2). After applying these criteria, a total of 65 patients were included in the final analysis.

Chemotherapy Regimens

All patients completed the prescribed systemic NAC and subsequently underwent surgery. NAC regimens were categorized into three distinct groups: anthracycline-based regimens (doxorubicin or epirubicin), taxane-based regimens (docetaxel or paclitaxel), and sequential regimens combining both anthracyclines and taxanes (Table 1). No patients received neoadjuvant endocrine therapy or radiotherapy.

Table 1. Clinical and pathological characteristics of the study cohort (n = 65)

Variable	Category	n	%
Lesion laterality	Left	34	52%
	Right	31	48%
Number of lesions	Unifocal	54	83%
	Multifocal	11	17%
Lesion distribution on MRI	Multicentric	7	11%
	Multifocal	10	15%
	Solitary	48	74%
MRI enhancement pattern	Mass enhancement	53	81%
	Non-mass enhancement	12	19%
Mid-NAC MRI radiological response	Radiologic complete response	8	12%
	Non-complete response	57	88%
Post-treatment radiological response	Radiologic complete response	25	38%
	Non-complete response	40	62%
Primary tumor pCR status	pCR	19	29%
	Non-pCR	46	71%
NAC regimen	Standard AC - taxane	3	5%
	Dose-dense AC - taxane	54	83%
	EC/FEC - taxane	6	9%
	Taxane-only	2	3%
Molecular subtype	Hormone receptor-positive	36	55%
	HER2-positive	17	26%
	Triple-negative	12	19%
Clinical T stage (cT)	cT1	10	15%
	cT2	44	68%
	cT3-T4	11	17%
Clinical nodal status (cN)	cN0	2	3%
	cN1	36	55%
	cN2-N3	27	42%
Tumor grade	1	4	6%
	2	34	52%
	3	27	42%

Table 1. Continued

Variable	Category	n	%
Surgical procedure	Partial mastectomy and SLNB	22	34%
	Total mastectomy and SLNB	5	8%
	Partial mastectomy and ALND	38	58%
Estrogen receptor status	Positive	48	74%
	Negative	17	26%
Progesterone receptor status	Positive	43	66%
	Negative	22	34%
Ki-67 proliferation index	<14	12	18%
	14–20	11	17%
	>20	42	65%

pCR: Pathologic complete response; SLNB: Sentinel lymph node biopsy; ALND: Axillary Lymph node dissection; AC: Adriamycin (doxorubicin) and cyclophosphamide; EC: Epirubicin and cyclophosphamide; FEC: 5-Fluorouracil, epirubicin, and cyclophosphamide; HER2: Human epidermal growth factor receptor 2; MRI: Magnetic resonance imaging; NAC: Neoadjuvant chemotherapy

Histopathological Evaluation

Breast tumor samples obtained through tru-cut biopsy were classified into three molecular subgroups based on immunohistochemical markers: hormone receptor–positive [estrogen receptor (ER) and/or progesterone receptor (PR) positive, HER2-negative], HER2-positive (regardless of hormone receptor status), and triple-negative (ER-negative, PR-negative, and HER2-negative). A tumor was considered hormone receptor–positive if either ER or PR showed ≥1% positivity on immunohistochemistry.

Following surgery, the response to NAC was assessed using the Miller–Payne grading system (Grade 1–5) (12). Grades 1 to 4 were classified as non-pCR, while Grade 5 was defined as pCR. The presence of ductal carcinoma *in situ* was excluded from the definition of pCR. Similarly, axillary nodal status was not considered in the pCR assessment.

MRI Technique

All breast MRI examinations were performed using a 1.5 Tesla scanner (Magnetom Aera, Siemens Healthineers, Erlangen, Germany) equipped with a dedicated breast coil. Imaging was conducted at three predefined time points: pre-NAC, mid-NAC (after the fourth chemotherapy cycle), and post-NAC. Mid-NAC MRI was performed at a mean of 8.4±1.8 weeks after the initiation of chemotherapy, with a median of 8.3 weeks [interquartile range (IQR): 7.3–9.5 weeks].

The standardized protocol included the following sequences in the axial plane: T1-weighted fat-saturated (TR/TE: 476/11 ms, slice thickness: 4.0 mm), T2-weighted turbo spin-echo (TR/TE: 6240/76 ms, slice thickness: 4.0 mm), turbo inversion recovery magnitude (TR/TE: 2250/56 ms), and T1-weighted Dixon (TR/TE: 449/11 ms). Diffusion-weighted imaging (DWI) was acquired using a single-shot echo-planar imaging sequence with b-values of 50, 500, and 800 s/mm² (TR/TE: 6900/66 ms, slice thickness: 4.0 mm). Dynamic contrast-enhanced (DCE) MRI was obtained using a 3D fat-saturated T1-weighted gradient-echo sequence (TR/TE: 4.53/1.82 ms, slice thickness: 2.0 mm). A gadolinium-based contrast agent (gadobutrol, Gadovist®; Bayer, Berlin, Germany) was administered intravenously at a dose of 0.1 mmol/kg, followed by a 20 mL saline flush at a rate of 3 mL/s. Five sequential post-contrast phases were acquired, each lasting 90 seconds, with the first acquisition centering k-space at approximately 1.5 minutes after injection.

All participants were provided informed consent before undergoing imaging.

Radiologic Response Evaluation

All MRI studies were reviewed in consensus by two radiologists with 8 and 23 years of experience, using dedicated workstations (Siemens Healthineers), blinded to the pathological outcomes. Radiological response to NAC was assessed according to RECIST 1.1 criteria (13). For multifocal or multicentric breast cancer, up to two target lesions—preferably the largest—were selected for serial measurements. Non-target lesions were qualitatively assessed but not quantitatively measured.

Radiologic complete response (rCR) was defined as the complete disappearance of all measurable lesions without any residual contrast enhancement. If a residual structure was observed at the tumor site, additional evaluation with DWI was performed. Lesions lacking contrast enhancement were still classified as complete response. Patients who did not fulfill these criteria were categorized as non-rCR.

For each target lesion, the longest diameter, the second-longest diameter, and the shortest diameter were recorded. Based on these dimensions, bidimensional size and tumor volume were calculated. Bidimensional size (cm²) was defined as the product of the longest and second-longest diameters. Tumor volume (cm³) was estimated using the ellipsoid formula:

Volume = (π/6) × longest diameter × second diameter × shortest diameter

Signal intensity (SI) measurements were obtained on both pre-NAC and mid-NAC DCE-MRI scans. Two key values were recorded: The baseline SI before contrast injection (SI_pre) and the peak SI during the early post-contrast phase, approximately two minutes after injection (SI_peak) (10, 14). The early peak enhancement (Epeak) was calculated using the formula:

Epeak (%) = [(SI_peak – SI_pre) / SI_pre] × 100

In patients with rCR, SI measurements on mid-NAC MRI were obtained from the anatomical location corresponding to the original tumor site.

ADC values were measured by placing circular regions of interest (ROIs) within the most diffusion-restricted area of each lesion, identified on high b-value DWI. ROIs were placed on the corresponding hypointense region on the ADC map to accurately reflect the most cellular portion of the tumor. Each ROI had a standardized area of 0.5 cm². Necrotic or cystic areas were carefully avoided, as they could artificially elevate ADC values (Figure 1). In rCR cases, ADC values were measured from the original tumor site on mid-NAC MRI. For patients with multifocal disease, the largest lesion was selected as the primary target for quantitative analysis.

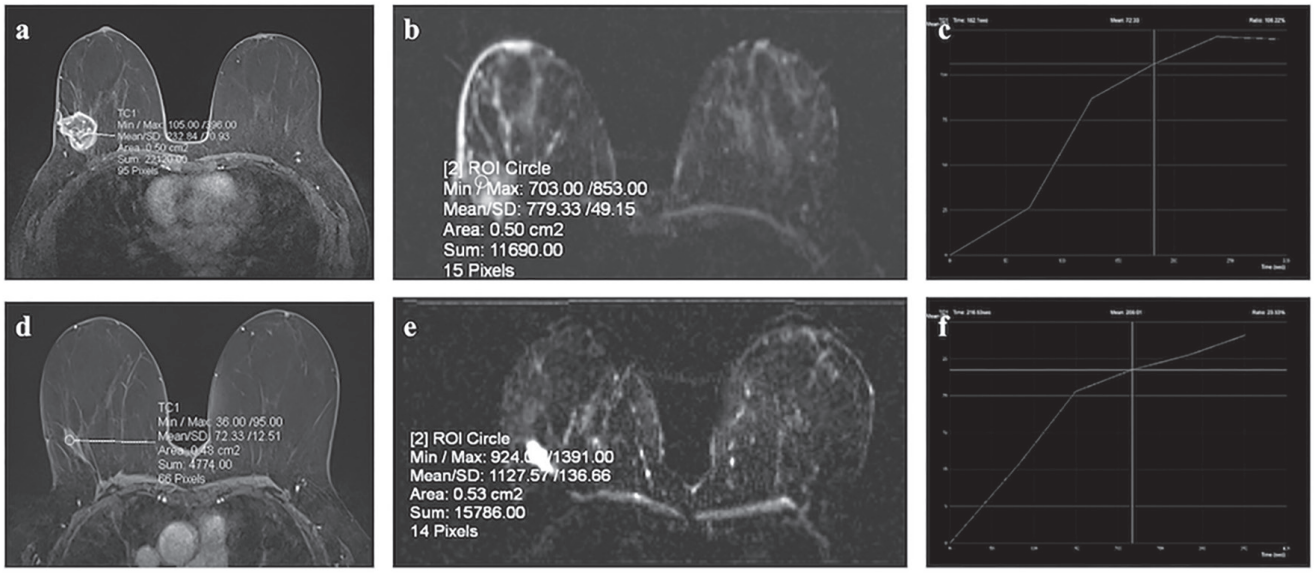

Figure 1. Pre- and mid- neoadjuvant chemotherapy (NAC) breast magnetic resonance imaging (MRI) of a 60-year-old woman with clinical stage cT2N1 triple-negative invasive ductal carcinoma who demonstrated a partial pathological response at the end of treatment, (a) axial post-contrast T1-weighted (T1W) image, (b) apparent diffusion coefficient (ADC) map, and (c) time–intensity curve (TIC) with calculated Epeak from the pre-NAC MRI, (d) axial post-contrast T1W image, (e) ADC map, and (f) TIC with Epeak from the mid-NAC MRI

All quantitative measurements were performed once per lesion without repetition.

Percentage changes (Δ%) in tumor dimensions and quantitative MRI parameters between pre-NAC and mid-NAC were calculated using the formula:

$$\Delta\% = [(Pre - Mid) / Pre] \times 100$$

Statistical Analysis

All statistical analyses were performed using SPSS version 26.0 (IBM Corp., Armonk, NY, USA). A two-tailed *p*-value of <0.05 was considered statistically significant. Categorical variables, including clinical and pathological characteristics, were summarized as frequencies and percentages. Continuous variables, such as tumor dimensions and MRI-derived parameters, were presented as mean ± standard deviation, median (minimum–maximum), and IQR (25^{th}–75^{th} percentiles). The Mann-Whitney U test was used to compare non-normally distributed variables between groups. Diagnostic performance was evaluated using receiver operating characteristic (ROC) curve analysis, and optimal cut-off values were determined using Youden's index. These thresholds were used to derive dichotomous variables for further analysis. Associations between radiologic parameters and pCR were assessed using Yates' corrected chi-square test or Fisher's exact test, depending on expected frequencies. Univariate logistic regression was used to calculate odds ratios (ORs) with corresponding 95% confidence intervals (CIs). Variables with statistical significance in univariate analysis were included in a multiple logistic regression (MLR) model using the backward stepwise (Wald) method. Model calibration was evaluated using the Hosmer-Lemeshow goodness-of-fit test, and multicollinearity among predictors was assessed to ensure the retention of independent variables. The assumption of normality was tested using the Shapiro-Wilk test and visual inspection of Q-Q plots. Pairwise comparisons of area under the curves (AUC) values between MRI parameters were performed using DeLong's test, a non-parametric method for comparing correlated ROC curves.

Results

The study cohort included 65 female breast cancer patients, with a mean age at diagnosis of 50±9 years (IQR: 44–56). pCR of the primary tumor was achieved in 19 patients (29%), while 46 patients (71%) were classified as non-pCR (Table 1).

Quantitative MRI analysis showed a marked reduction in tumor dimensions and enhancement characteristics from pre- to mid-NAC. The mean longest diameter decreased from 3.47±1.77 cm to 2.08±1.48 cm, with a mean percent change (Δ%) of 40%. Tumor volume decreased from 17.6±36.3 cm^3 to 5.4±17.7 cm^3 (Δ%: 71%). Epeak declined from 177±101% to 100±79% (Δ%: 23%), while ADC values increased from 867±180 to 1035±148 $\times 10^{-6}$ mm^2/s (Δ%: -23%) (Table 2). Notably, due to the calculation formula [(Pre – Mid) / Pre × 100], negative Δ% ADC values indicate an actual increase in ADC.

Patients who achieved pCR exhibited significantly greater reductions in tumor size and enhancement metrics on mid-NAC MRI. The mean percent decrease (Δ%) in longest diameter, second diameter, shortest diameter, tumor volume, and bidimensional size was significantly higher in the pCR group compared to non-pCR (all $p<0.01$) (Table 3). Notably, mid-NAC ADC values were significantly higher (1107 vs. 1006 $\times 10^{-6}$ mm^2/s, $p = 0.015$), and mid-NAC Epeak values were lower (68 vs. 113%, $p = 0.007$) in patients with pCR.

ROC analysis demonstrated that several mid-NAC MRI-based parameters had good discriminatory ability for predicting pCR (Table 4, Figure 2). Δ% longest diameter >60% achieved an AUC of 0.740 (95% CI: 0.616–0.841) with high specificity (91%). Δ% second diameter >46% provided the highest sensitivity (74%) with 70% specificity (AUC=0.752; 95% CI: 0.630–0.851). Tumor volume reduction >92% also showed strong performance with an AUC of 0.754 (95% CI: 0.631–0.852) and specificity of 89%. Among functional metrics, Epeak ≤21% yielded perfect specificity (100%) with an AUC of 0.715 (95% CI: 0.590–0.820), although sensitivity

Table 2. Descriptive statistics of tumor dimensions and radiologic MRI parameters (*n* = 65)

Parameter	Mean ± SD	Median (min-max)	Percentile (25–75)
Longest diameter (cm)			
- Pre-NAC MRI	3.47±1.77	3.1 (0.94–9.7)	(2.38–4.1)
- Mid-NAC MRI	2.08±1.48	1.9 (0.0–7.5)	(1.4–2.8)
- Δ%	40±30	32 (-6–100)	(16–56)
Second diameter (cm)			
- Pre-NAC MRI	2.72±1.28	2.43 (0.93–8.7)	(2.0–3.29)
- Mid-NAC MRI	1.5±1.08	1.5 (0.0–6.3)	(0.81–2.1)
- Δ%	45±30	41 (-7–100)	(24–61)
Shortest diameter (cm)			
- Pre-NAC MRI	2.11±0.96	1.9 (0.83–6.2)	(1.5–2.46)
- Mid-NAC MRI	1.15±0.87	1.0 (0.0–5.6)	(0.6–1.5)
- Δ%	46±30	42 (-10–100)	(26–64)
Bidimensional size (cm^2)			
- Pre-NAC MRI	11.4±12.6	7.5 (0.87–84.4)	(4.5–13.9)
- Mid-NAC MRI	4.6±6.9	3.0 (0–47.3)	(1.3–5.0)
- Δ%	59±29	61 (-8–100)	(43–82)
Tumor volume (cm^3)			
- Pre-NAC MRI	17.6±36.3	7.2 (0.4–273.6)	(3.9–17.1)
- Mid-NAC MRI	5.4±17.7	1.5 (0–138.4)	(0.4–4.6)
- Δ%	71±27	79 (-18–100)	(53–92)
Pre-contrast SI			
- Pre-NAC MRI	201±61	201 (59–380)	(163–238)
- Mid-NAC MRI	196±57	208 (73–301)	(150–250)
- Δ%	-3±32	1 (-81–65)	(-18–15)
Post-contrast peak SI			
- Pre-NAC MRI	527±174	537 (156–908)	(380–648)
- Mid-NAC MRI	377±141	347 (149–750)	(269–471)
- Δ%	23±30	25 (-48–76)	(0–48)
Epeak (%)			
- Pre-NAC MRI	177±101	165 (32–441)	(86–248)
- Mid-NAC MRI	100±79	83 (0–350)	(46–126)
- Δ%	23±82	47 (-422–100)	(3–72)
ADC value (×10⁻⁶ mm^2/s)			
- Pre-NAC MRI	867±180	849 (421–1587)	(726–970)
- Mid-NAC MRI	1035±148	1025 (730–1360)	(950–1154)
- Δ%	-23±27	-20 (-125–32)	(-39 – -7)

SD: Standard deviation; NAC: Neoadjuvant chemotherapy; SI: Signal intensity; ADC: Apparent diffusion coefficient; Δ%: Percent change from pre- to mid-NAC MRI; calculated as [(Pre – Mid) / Pre] × 100, Negative Δ% ADC values represent ADC increase; MRI: Magnetic resonance imaging; min: Minimum; max: Maximum

Table 3. Comparison of pre- and mid-NAC MRI-based quantitative parameters by pCR status

Parameter	pCR (n = 19)		Non-pCR (n = 46)		
	Mean ± SD	Median (IQR)	Mean ± SD	Median (IQR)	*p*-value
Longest diameter (cm)					
- Pre-NAC MRI	3.2±1.4	3.1 (2.4)	3.6±1.9	3.1 (1.5)	0.812
- Mid-NAC MRI	1.4±1.4	1.4 (2.5)	2.4±1.4	2.0 (1.3)	0.013*
- Δ%	60±34	55 (69)	32±25	30 (31)	0.002*
Second diameter (cm)					
- Pre-NAC MRI	2.6±1.0	2.5 (1.2)	2.8±1.4	2.4 (1.3)	0.977
- Mid-NAC MRI	1.0±0.9	0.9 (1.8)	1.7±1.1	1.6 (1.1)	0.009*
- Δ%	64±32	63 (65)	36±25	35 (40)	0.001*
Shortest diameter (cm)					
- Pre-NAC MRI	2.0±0.7	2.0 (1.0)	2.2±1.0	1.9 (1.0)	0.660
- Mid-NAC MRI	0.7±0.7	0.5 (1.5)	1.3±0.9	1.2 (0.7)	0.016*
- Δ%	66±30	63 (65)	38±26	39 (34)	0.003*
Bidimensional size (cm^2)					
- Pre-NAC MRI	9.5±6.8	7.5 (10.4)	12.1±14.3	7.3 (8.7)	0.988
- Mid-NAC MRI	2.5±3.2	1.3 (4.5)	5.4±7.7	3.2 (5.0)	0.014*
- Δ%	77±24	85 (54)	52±28	53 (43)	0.001*
Tumor volume (cm^3)					
- Pre-NAC MRI	11.6±10.7	8.3 (13.2)	20.1±42.5	7.2 (14.8)	0.806
- Mid-NAC MRI	1.9±2.9	0.3 (3.5)	6.9±20.8	2.2 (4.1)	0.013*
- Δ%	86±17	95 (29)	65±28	71 (40)	0.001*
Pre-contrast SI					
- Pre-NAC MRI	199±53	199 (87)	202±65	202 (76)	0.829
- Mid-NAC MRI	208±56	210 (100)	192±57	207 (91)	0.299
- Δ%	-10±36	-11 (47)	0±30	2 (27)	0.240
Post-contrast peak SI					
- Pre-NAC MRI	495±166	485 (280)	540±177	548 (260)	0.330
- Mid-NAC MRI	336±142	289 (221)	393±139	393 (172)	0.102
- Δ%	24±39	40 (69)	23±26	24 (41)	0.593
Epeak (%)					
- Pre-NAC MRI	159±99	117 (157)	185±102	173 (165)	0.364
- Mid-NAC MRI	68±75	60 (92)	113±77	92 (71)	0.007*
- Δ%	32±86	70 (93)	20±80	41 (55)	0.087
ADC value ($\times 10^{-6}$ mm^2/s)					
- Pre-NAC MRI	865±156	888 (251)	867±191	848 (246)	0.96
- Mid-NAC MRI	1107±128	1120 (219)	1006±147	1002 (164)	0.015*
- Δ%	-31±26	-35 (35)	-20±26	-16 (23)	0.060

SD: Standard deviation; IQR: Interquartile range (25^{th}–75^{th}); SI: Signal intensity; NAC: Neoadjuvant chemotherapy; ADC: Apparent diffusion coefficient; pCR: Pathologic complete response; Δ%: Percent change from pre- to mid-NAC MRI, calculated as [(Pre – Mid) / Pre] × 100. Negative Δ% ADC values represent ADC increase; *: $p<0.05$ indicates statistical significance; MRI: Magnetic resonance imaging

was lower (37%). Most dimensional parameters achieved AUC values >0.73 (p<0.01), supporting their predictive utility (Table 4).

Pairwise comparisons of AUC values between Δ% MRI parameters—including diameters, bidimensional size, tumor volume, and ADC—showed no significant differences (all p>0.05). Δ% dimensional metrics demonstrated highly similar performance (AUC differences <0.015), while Δ% ADC tended to yield slightly higher AUCs without reaching significance (Supplementary Table 1).

Binary analysis based on optimal cut-off values confirmed significant associations between mid-NAC MRI–derived parameters and pCR (Table 5). Patients with Δ% longest diameter >60%, second diameter >46%, shortest diameter >45%, or tumor volume reduction >92% had significantly higher rates of pCR (all p<0.01). Additionally, patients with Epeak ≤21% and Δ% ADC value ≥32% showed significantly higher pCR rates (p<0.01 for both).

In univariable analysis, multiple mid-NAC MRI–based parameters were significantly associated with pCR, including Δ% longest diameter >60% (OR=9.5; 95% CI: 2.4–37.0; p = 0.001), Δ% ADC value ≥32% (OR=6.2; 95% CI: 1.9–19.8; p = 0.003), and Δ% tumor volume >92% (OR=5.3; 95% CI: 1.6–17.2; p = 0.010) (Table 6). Epeak ≤21% demonstrated the highest univariable OR (OR=26.3; 95% CI: 2.9–234.5; p<0.001) but was excluded from the MLR model due to wide CIs indicating model instability. Δ% second diameter, shortest diameter, and bidimensional size also showed significant associations (all p<0.01) but were excluded due to collinearity.

In the final MLR model, only Δ% longest diameter >60% (OR=7.1; 95% CI: 1.3–30.1; p = 0.008) and Δ% ADC value ≥32% (OR=4.7; 95% CI: 1.3–16.5; p = 0.016) remained as independent predictors of pCR (Table 6). The model excluded redundant or unstable variables, favoring robust and non-collinear biomarkers. Overall model performance was acceptable (Nagelkerke R^2 = 0.336), with good calibration (Hosmer-Lemeshow p = 0.800).

Discussion and Conclusion

In the overall cohort, all dimensional MRI parameters showed a mean reduction from pre- to mid-NAC, while mean post-contrast SI, Epeak, decreased and mean ADC values increased, consistent with early treatment response (Table 2). Furthermore, comparison between pCR and non-pCR groups revealed significantly greater reductions in longest diameter, second and shortest diameters, bidimensional size, and tumor volume, as well as lower mid-treatment Epeak and higher ADC values in the pCR cohort (all p<0.05, Table 3). These differences underscore the utility of both morphologic and functional MRI parameters in distinguishing responders from non-responders during mid-NAC assessment, in line with prior studies that demonstrated the predictive value of early volumetric reduction and diffusion changes for pCR (7, 8, 11).

As shown in Table 3, pre-contrast SI on mid-NAC MRI exhibited a slight increase in the pCR group, whereas it remained stable or decreased in the non-pCR group; however, this difference did not reach statistical significance. This observation may be explained by treatment-induced stromal alterations such as proteinaceous or hemorrhagic content, fibrosis, and necrotic debris, which shorten T1 relaxation time and elevate SI despite fat suppression. Nevertheless, given its limited clinical relevance, this parameter should not be considered a primary predictor of therapeutic response.

Univariable ROC analysis revealed that several morphologic and functional MRI parameters demonstrated significant predictive performance for pCR. Among dimensional metrics, tumor volume reduction >92% achieved the highest AUC (0.754), followed closely by bidimensional size >69% (AUC=0.752) and longest diameter >60% (AUC=0.740). Notably, the >60% reduction in the longest diameter yielded the highest specificity (91%), suggesting its utility in identifying true responders, whereas bidimensional shrinkage provided the highest sensitivity (74%), making it more suitable for screening purposes. These findings are in agreement with prior work by Fangberget et al. (15), who demonstrated that tumor volume

Table 4. ROC analysis of radiologic features on mid-NAC MRI for predicting pCR

Parameter	AUC (95% CI)	p-value (area=0.5)	Youden's J	Cut-off value	Sensitivity (%)	Specificity (%)
Δ% Longest diameter	0.740 (0.616–0.841)	<0.001**	0.39	>60%	47	91
Δ% Second diameter	0.752 (0.630–0.851)	0.001**	0.43	>46%	74	70
Δ% Shortest diameter	0.739 (0.615–0.840)	0.001**	0.41	>45%	74	67
Δ% Bidimensional size	0.752 (0.629–0.851)	<0.001**	0.42	>69%	68	74
Δ% Tumor volume	0.754 (0.631–0.852)	<0.001**	0.42	>92%	53	89
Epeak	0.715 (0.590–0.820)	0.006**	0.37	≤21	37	100
Δ% Pre-contrast SI	0.593 (0.464–0.713)	0.267	0.27	≤-10%	58	70
Δ% Post-contrast SI	0.542 (0.414–0.667)	0.649	0.23	>45%	47	76
Δ% Epeak	0.636 (0.507–0.751)	0.138	0.34	>73%	47	87
Δ% ADC value	0.649 (0.521–0.764)	0.071	0.41	≥32%	63	78

AUC: Area under the curve; CI: Confidence interval; ADC: Apparent diffusion coefficient; SI: Signal intensity; Δ%: Percent change from pre- to mid-NAC MRI, calculated as [(Pre – Mid) / Pre] × 100; Optimal cut-off values were determined using Youden's index (J); **: p<0.01 (statistically significant); NAC: Neoadjuvant chemotherapy; pCR: Pathologic complete response; MRI: Magnetic resonance imaging

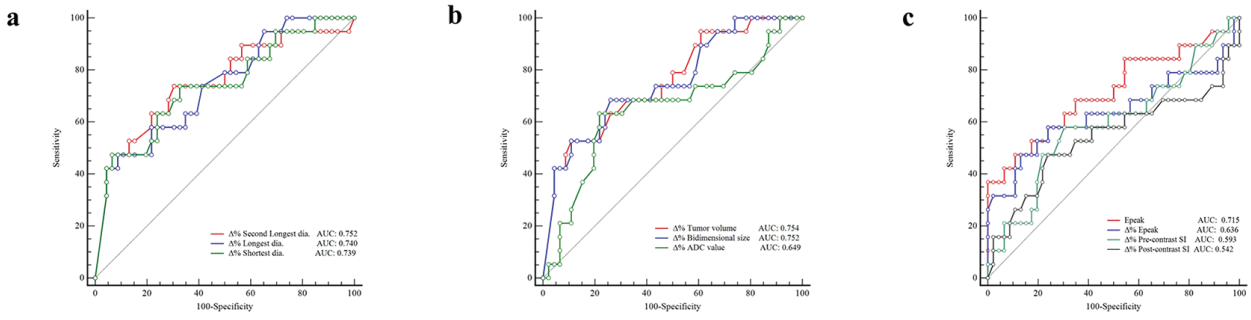

Figure 2. Receiver operating characteristic curves of mid-treatment magnetic resonance imaging parameters for predicting pathologic complete response, (a) Δ% second longest diameter [area under the curve (AUC)=0.752], Δ% longest diameter (AUC=0.740), Δ% shortest diameter (AUC=0.739), (b) Δ% tumor volume (AUC=0.754), Δ% bidimensional size (AUC=0.752), Δ% apparent diffusion coefficien value (AUC=0.649), (c) Epeak (AUC=0.715), Δ% Epeak (AUC=0.636), Δ% pre-contrast SI (AUC=0.593), Δ% post-contrast SI (AUC=0.542)

Table 5. Association between mid-NAC MRI-based radiologic parameters and pCR status (*n* = 65)

Parameter (cut-off value)	pCR (n = 19)	Non-pCR (n = 46)	*p*-value
Δ% Longest diameter			
>60%	9 (47.4%)	4 (8.7%)	0.001**
≤60%	10 (52.6%)	42 (91.3%)	
Δ% Second diameter			
>46%	14 (73.7%)	14 (30.4%)	0.003*
≤46%	5 (26.3%)	32 (69.6%)	
Δ% Shortest diameter			
>45%	14 (73.7%)	15 (32.6%)	0.006*
≤45%	5 (26.3%)	31 (67.4%)	
Δ% Bidimensional size			
>69%	13 (68.4%)	12 (26.1%)	0.004*
≤69%	6 (31.6%)	34 (73.9%)	
Δ% Tumor volume			
>92%	10 (52.6%)	8 (17.4%)	0.010*
≤92%	9 (47.4%)	38 (82.6%)	
Δ% ADC value			
≥32%	12 (63.2%)	10 (21.7%)	0.003*
<32%	7 (36.8%)	36 (78.3%)	
Epeak (%)			
≤21	7 (36.8%)	1 (2.2%)	<0.001**
>21	12 (63.2%)	45 (97.8%)	

Δ%: Percent change from pre- to mid-NAC MRI, calculated as [(Pre – Mid) / Pre] × 100; ADC: Apparent diffusion coefficient; pCR: Pathologic complete response. Group comparisons were made using chi-square or Fisher's exact test; $p<0.05$ was considered statistically significant (*); $p<0.01$ was considered highly significant (**); MRI: Magnetic resonance imaging; NAC: Neoadjuvant chemotherapy

reduction ≥83% after four cycles of NAC was the most accurate predictor of pCR, with a sensitivity of 91%, specificity of 80%, and AUC of 0.82, outperforming longest diameter reduction (AUC=0.78). This supports the notion that while unidimensional measures like longest diameter remain clinically useful, volumetric assessment better reflects the complex and often irregular patterns of tumor regression during NAC. Conversely, Minarikova et al. (16) reported that 3D diameter change outperformed volume metrics (AUC=0.933), suggesting that diameter-based measurements may offer better practicality and performance in certain clinical settings. In our cohort, however, pairwise AUC comparisons showed no statistically significant differences between Δ% longest diameter, bidirectional size, and tumor volume (all $p>0.05$), indicating comparable predictive performance across these morphologic parameters.

In the MLR analysis, Δ% longest diameter >60% (OR=7.1, $p = 0.008$) and Δ% ADC value ≥32% (OR=4.7, $p = 0.016$) emerged as the only independent predictors of pCR. These findings reinforce

Table 6. Univariable and multiple logistic regression analysis of Mid-NAC MRI-based parameters for pCR prediction

Parameter (Δ%, mid-NAC MRI)		Univariable analysis		Multivariable analysis (final model)		
		OR (95% CI)	p	OR (95% CI)	p	Model inclusion status
Δ% Longest diameter	>60%	9.5 (2.4–37.0)	0.001	7.1 (1.3–30.1)	0.008	Retained
Δ% ADC value	≥32%	6.2 (1.9–19.8)	0.003	4.7 (1.3–16.5)	0.016	Retained
Δ% Tumor volume	>92%	5.3 (1.6–17.2)	0.010	–	0.869	Dropped at Step2
Δ% Second diameter	>46%	6.4 (1.9–21.2)	0.003	–	–	Not selected
Δ% Shortest diameter	>45%	5.8 (1.8–19.1)	0.006	–	–	Not selected
Δ% Bidimensional size	>69%	6.1 (1.9–19.8)	0.004	–	–	Not selected
Epeak (%)	≤21	26.3 (2.9–234.5)	<0.001	–	–	Not selected

OR: Odds ratio; CI: Confidence interval; pCR: Pathologic complete response; ADC: Apparent diffusion coefficient; Δ%: Percent change from pre- to mid-NAC MRI, calculated as [(Pre – Mid) / Pre] × 100; the multiple logistic regression model was constructed using backward stepwise (Wald) method. Nagelkerke R^2=0.336; Hosmer-Lemeshow test p = 0.800; Constant = -1.995; MRI: Magnetic resonance imaging; NAC: Neoadjuvant chemotherapy

the complementary value of morphologic shrinkage and diffusion metrics in early treatment monitoring. While other dimensional parameters also showed strong univariable associations with pCR, they were excluded from the final model due to collinearity. Notably, Δ% tumor volume >92%—despite having the highest univariable AUC (0.754)—lost significance in MLR analysis (p = 0.869), likely reflecting overlapping predictive information with longest diameter and ADC changes. This emphasizes the importance of selecting non-collinear and stable parameters for robust modeling in clinical practice.

The increase in ADC values, reflected by Δ% ADC ≥32%, suggests reduced tumor cellularity in response to effective cytotoxic therapy. Chemotherapy-induced necrosis and decreased cell density enhance water diffusivity, which is captured by ADC elevation on DW-MRI (17, 18). In our cohort, both higher mid-NAC ADC values and greater percent increases were significantly associated with pCR, consistent with prior findings from both multicenter and single-institution studies, supporting ADC as a reliable non-invasive biomarker of treatment response (7, 11). In contrast to prior multicenter studies such as ACRIN 6698, which demonstrated moderate predictive performance for mid-treatment ΔADC without specifying an optimal cut-off (AUC=0.60), our study identified a Δ% ADC ≥32% as an independent predictor of pCR with higher specificity and multivariable significance (7). Similarly, a recent multi-institutional study on HER2-positive breast cancer also reported ΔADC as a significant early predictor of treatment response (19).

Similarly, lower mid-NAC Epeak values—particularly those ≤21%—were highly specific for pCR (100%), although their predictive utility was limited by low sensitivity (37%) and instability in MLR modeling. As a semi-quantitative indicator of early contrast enhancement kinetics, Epeak reflects tumor vascularity and perfusion. A pronounced decline in Epeak following chemotherapy may correspond to reduced angiogenic activity, vessel permeability, and microvascular density, consistent with a strong cytotoxic effect. In our cohort, both lower absolute mid-NAC Epeak values and greater percent reductions were significantly associated with pCR in univariable analysis. These findings are in line with previous studies suggesting that early changes in perfusion-related parameters may signal effective treatment response. Supporting this, one recent study demonstrated that greater reductions in early peak enhancement during NAC were associated with favorable pathological response and improved recurrence-free survival (20). Additionally, a large retrospective cohort of 168 breast cancer patients reported that both pre-NAC Epeak ≤96 and post-NAC Epeak >188 were independent predictors of pCR and survival outcomes, further underscoring the prognostic value of contrast enhancement dynamics during treatment (10).

From a clinical perspective, the integration of early mid-treatment MRI biomarkers—particularly Δ% longest diameter and Δ% ADC—offers a practical and non-invasive strategy to identify patients who are likely to achieve pCR during NAC. These parameters can be easily derived from routine clinical MRI protocols without the need for advanced post-processing or pharmacokinetic modeling, increasing their feasibility in everyday practice. The high specificity of Δ% longest diameter >60% and the independent predictive value of Δ% ADC ≥32% support their utility in guiding individualized treatment decisions. For instance, patients demonstrating suboptimal early imaging response may be candidates for treatment intensification or alternative therapeutic strategies, while early identification of good responders may inform ongoing monitoring or risk stratification efforts. Thus, the use of accessible imaging biomarkers to differentiate responders from non-responders at an early stage may support more personalized and adaptive approaches in breast cancer management.

Study Limitations

This study has several limitations. First, its retrospective design and single-center setting may limit the generalizability of the findings. Second, the sample size—though adequate for exploratory modeling—was relatively modest, particularly for MLR, which may affect the stability of certain parameters, such as Epeak. Third, manual ROI placement for ADC and enhancement measurements, although performed in consensus by experienced radiologists, may introduce variability and operator dependence. Additionally, Epeak, as a semi-quantitative measure, is susceptible to temporal resolution and sequence timing, which could limit reproducibility across different imaging protocols. Moreover, the lack of inter-reader reproducibility testing further limits generalizability.

Mid-treatment MRI biomarkers—including Δ% longest diameter and Δ% ADC—demonstrated significant predictive value for pCR in patients undergoing NAC for LABC. These easily obtainable and non-

invasive parameters may serve as reliable early indicators of treatment response, potentially enabling more personalized therapeutic strategies in clinical practice.

Ethics

Ethics Committee Approval: This retrospective study was approved by the University of Health Sciences Türkiye, İzmir Bozyaka Training and Research Hospital Clinical Research Ethics Committee (approval date: 29/11/2023; decision no: 2023/197).

Informed Consent: All participants were provided informed consent before undergoing imaging.

Footnotes

Authorship Contributions

Surgical and Medical Practices: A.B., L.A.; Concept: A.B., H.E.G.; Design: L.A., H.E.G.; Data Collection or Processing: A.B., H.E.G.; Analysis or Interpretation: L.A.; Literature Search: A.B., L.A.; Writing: A.B.

Conflict of Interest: No conflict of interest was declared by the authors.

Financial Disclosure: The authors declared that this study received no financial support.

References

1. Spring LM, Fell G, Arfe A, Sharma C, Greenup R, Reynolds KL, et al. Pathologic complete response after neoadjuvant chemotherapy and impact on breast cancer recurrence and survival: a comprehensive meta-analysis. Clin Cancer Res. 2020; 26: 2838-2848. (PMID: 32046998) [Crossref]
2. Cortazar P, Zhang L, Untch M, Mehta K, Costantino JP, Wolmark N, et al. Pathological complete response and long-term clinical benefit in breast cancer: the CTNeoBC pooled analysis. Lancet. 2014; 384: 164-172. (PMID: 24529560) Erratum in: Lancet. 2019; 393: 986. [Crossref]
3. Park J, Chae EY, Cha JH, Shin HJ, Choi WJ, Choi YW, et al. Comparison of mammography, digital breast tomosynthesis, automated breast ultrasound, magnetic resonance imaging in evaluation of residual tumor after neoadjuvant chemotherapy. Eur J Radiol. 2018; 108: 261-268. (PMID: 30396666) [Crossref]
4. Romeo V, Accardo G, Perillo T, Basso L, Garbino N, Nicolai E, et al. Assessment and prediction of response to neoadjuvant chemotherapy in breast cancer: a comparison of imaging modalities and future perspectives. Cancers (Basel). 2021; 13: 3521. (PMID: 34298733) [Crossref]
5. Sudhir R, Koppula V, Mandava A, Kamala S, Potlapalli A. Technique and clinical applications of dual-energy contrast-enhanced digital mammography (CEDM) in breast cancer evaluation: a pictorial essay. Diagn Interv Radiol. 2021; 27: 28-36. (PMID: 33252334) [Crossref]
6. Taydaş O, Durhan G, Akpınar MG, Demirkazık FB. Comparison of MRI and US in tumor size evaluation of breast cancer patients receiving neoadjuvant chemotherapy. Eur J Breast Health. 2019; 15: 119-124. (PMID: 31001614) [Crossref]
7. Partridge SC, Zhang Z, Newitt DC, Gibbs JE, Chenevert TL, Rosen MA, et al; ACRIN 6698 Trial Team and I-SPY 2 Trial Investigators. Diffusion-weighted MRI findings predict pathologic response in neoadjuvant treatment of breast cancer: the ACRIN 6698 multicenter trial. Radiology. 2018; 289: 618-627. (PMID: 30179110) [Crossref]
8. Tudorica A, Oh KY, Chui SY, Roy N, Troxell ML, Naik A, et al. Early prediction and evaluation of breast cancer response to neoadjuvant chemotherapy using quantitative DCE-MRI. Transl Oncol. 2016; 9: 8-17. (PMID: 26947876) [Crossref]
9. Park SH, Moon WK, Cho N, Song IC, Chang JM, Park IA, et al. Diffusion-weighted MR imaging: pretreatment prediction of response to neoadjuvant chemotherapy in patients with breast cancer. Radiology. 2010; 257: 56-63. (PMID: 20851939) [Crossref]
10. Bozer A, Yilmaz C, Çetin Tunçez H, Kocatepe Çavdar D, Adıbelli ZH. MR imaging features predictive of pathologic complete response and survival outcomes for breast cancer patients undergoing neoadjuvant chemotherapy. Magn Reson Med Sci. 2025 Mar 15. (PMID: 40090737) [Crossref]
11. Le-Petross H, Son JB, Ma J, Kai M, Whitman G, Guirguis M, et al. Abstract P4-05-23: quantitative diffusion weighted imaging for predicting response to neoadjuvant therapy in patients with inflammatory breast cancer. Clin Cancer Res. 2025; 31(12 Suppl): P4-05-23. [Crossref]
12. Ogston KN, Miller ID, Payne S, Hutcheon AW, Sarkar TK, Smith I, et al. A new histological grading system to assess response of breast cancers to primary chemotherapy: prognostic significance and survival. Breast. 2003; 12: 320-327. (PMID: 14659147) [Crossref]
13. Eisenhauer EA, Therasse P, Bogaerts J, Schwartz LH, Sargent D, Ford R, et al. New response evaluation criteria in solid tumours: revised RECIST guideline (version 1.1). Eur J Cancer. 2009; 45: 228-247. (PMID: 19097774) [Crossref]
14. Rahbar H, Partridge SC. Multiparametric MR imaging of breast cancer. Magn Reson Imaging Clin N Am. 2016; 24: 223-238. (PMID: 26613883) [Crossref]
15. Fangberget A, Nilsen LB, Hole KH, Holmen MM, Engebraaten O, Naume B, et al. Neoadjuvant chemotherapy in breast cancer-response evaluation and prediction of response to treatment using dynamic contrast-enhanced and diffusion-weighted MR imaging. Eur Radiol. 2011; 21: 1188-1199. (PMID: 21127880) [Crossref]
16. Minarikova L, Bogner W, Pinker K, Valkovič L, Zaric O, Bago-Horvath Z, et al. Investigating the prediction value of multiparametric magnetic resonance imaging at 3 T in response to neoadjuvant chemotherapy in breast cancer. Eur Radiol. 2017; 27: 1901-1911. (PMID: 27651141) [Crossref]
17. Li X, Abramson RG, Arlinghaus LR, Kang H, Chakravarthy AB, Abramson VG, et al. Multiparametric magnetic resonance imaging for predicting pathological response after the first cycle of neoadjuvant chemotherapy in breast cancer. Invest Radiol. 2015; 50: 195-204. (PMID: 25360603) [Crossref]
18. Liang X, Chen X, Yang Z, Liao Y, Wang M, Li Y, et al. Early prediction of pathological complete response to neoadjuvant chemotherapy combining DCE-MRI and apparent diffusion coefficient values in breast Cancer. BMC Cancer. 2022; 22: 1250. (PMID: 36460972) [Crossref]
19. Chen S, Zheng B, Tang W, Ding S, Sui Y, Yu X, et al. The longitudinal changes in multiparametric MRI during neoadjuvant chemotherapy can predict treatment response early in patients with HER2-positive breast cancer. Eur J Radiol. 2024; 178: 111656. (PMID: 39098252) [Crossref]
20. Kazerouni AS, Peterson LM, Jenkins I, Novakova-Jiresova A, Linden HM, Gralow JR, et al. Multimodal prediction of neoadjuvant treatment outcome by serial FDG PET and MRI in women with locally advanced breast cancer. Breast Cancer Res. 2023; 25: 138. (PMID: 37946201) [Crossref]

Click the link to access Supplementary Tables 1: https://d2v96fxpocvxx.cloudfront.net/66b874bd-7aaa-4f61-9199-52f558d61c0d/content-images/6716ba7a-d906-4837-9552-1208353508c0.pdf